



## MiR-26a-5p exerts its influence by targeting EP300, a molecule known for its role in activating the PI3K/AKT/mTOR signaling pathway in CD8<sup>+</sup>tumor-infiltrating lymphocytes of colorectal cancer

Chao Wang<sup>1,2,3#</sup>, Haonan Lin<sup>1,2,3#</sup>, Wangqiang Zhao<sup>1,2,3</sup>, Yixuan Liang<sup>1,2,3</sup>, Yao Chen<sup>1,3</sup>, Changmiao Wang<sup>1,3\*</sup>

<sup>1</sup>Department of General Surgery, the First Affiliated Hospital of Dalian Medical University, Dalian, China

<sup>2</sup>Laboratory of Integrative Medicine, the First Affiliated Hospital of Dalian Medical University, Dalian, China

<sup>3</sup>Dalian Medical University, Dalian, China

#Chao Wang and Haonan Lin contributed equally to this work.

### ARTICLE INFO

#### Original paper

#### Article history:

Received: June 26, 2023

Accepted: September 24, 2023

Published: November 30, 2023

#### Keywords:

Colorectal cancer, tumor-infiltrating lymphocytes, miR-26a-5p, EP300, PI3K/AKT/mTOR, apoptosis

### ABSTRACT

Surgical resection remains the primary approach for treating colorectal cancer, which is among the prevalent types of cancers affecting the digestive system. Tumor-infiltrating lymphocyte (TIL) therapy has emerged as a prominent area of study in the field of tumor immunotherapy in recent times, with the potential to serve as a supplementary treatment for colorectal cancer. For this investigation, we employed single-cell sequencing data to assess the manifestation extent of miR-26a-5p in healthy colon tissue, tissue affected by colorectal cancer, and tissue adjacent to the tumor. According to our findings, tumor-infiltrating T lymphocytes express comparatively less miR-26a-5p in comparison to normal T lymphocytes, the role of it in modulating the function of tumor-infiltrating T lymphocytes is suggested. Studies on miR-26a-5p's involvement in tumor-infiltrating T lymphocytes are limited, despite previous evidence indicating its ability to facilitate the development and advancement of cancerous cells. As a result of our experiments, we concluded that miR-26a-5p hindered the PI3K/AKT/mTOR(PAM) signaling pathway, reducing the ability of CD8<sup>+</sup> tumor-infiltrating cells to eradicate tumors. Using bioinformatics tools, we utilized prediction methods to identify EP300 as the specific gene targeted by miR-26a-5p. Subsequent research understood that down-regulation of EP300 counteracted the suppressive impact exerted by miR-26a-5p on the stimulation of PAM signaling pathway, while it also diminished the viability and cytotoxicity of CD8<sup>+</sup> tumor-infiltrating lymphocytes. Therefore, miR-26a-5p emerges as a compelling option for the effective control of TIL therapy.

Doi: <http://dx.doi.org/10.14715/cmb/2023.69.12.37>

Copyright: © 2023 by the C.M.B. Association. All rights reserved.

### Introduction

Globally, colorectal cancer stands as one of the most prevalent malignancies affecting the digestive system. Recent data from the American Cancer Society in 2022 highlights the significant impact of colorectal cancer, ranking it as the third most common and fatal type of cancer. This underscores the immense public health risk it poses (1). While the intricate mechanisms behind the development of colorectal cancer remain incompletely understood, the interplay of both genetic predisposition and environmental factors is recognized as contributing to its onset. Presently, surgical intervention remains the cornerstone of colorectal cancer treatment. Complementary to surgery, chemotherapy and radiotherapy are employed to enhance therapeutic efficacy (2). However, a prominent challenge in the management of colorectal cancer lies in postoperative metastasis, a leading cause of treatment failure. This encompasses diverse forms such as blood-borne, peritoneal, and distant lymph node metastases, frequently accompanied by local recurrences. Despite a general decline in the overall fatality rate of colorectal cancer in recent years, a troubling trend

of increasing fatality rates among younger individuals has emerged. This alarming pattern emphasizes the pressing need to explore novel avenues for treatment. In light of the aforementioned context, there exists an imperative to innovate beyond established treatment modalities. Emerging therapies that target specific molecular pathways, harness the immune system, or utilize advanced technologies like precision medicine offer promise in reshaping the colorectal cancer treatment landscape. Additionally, comprehensive approaches focusing on early detection through advanced screening methods, coupled with lifestyle interventions to mitigate risk factors, hold potential to make substantial strides in preventing and managing this formidable disease. Efforts to unravel the intricacies of colorectal cancer's underlying biology, combined with the development of more effective and tailored therapies, are pivotal in addressing the evolving challenges posed by this disease. By fostering interdisciplinary collaboration, advancing research, and advocating for widespread awareness, the medical community can aspire to usher in a new era of improved outcomes and enhanced quality of life for those affected by colorectal cancer.

\* Corresponding author. Email: [wcmdyyy@163.com](mailto:wcmdyyy@163.com)

The tumor microenvironment (TME) encompasses a diverse array of cellular components, comprising either tumor cells and non-tumor components, for example, immune cells, endothelial cells, adipocytes, and fibroblasts are all present in the TME (3). These cells have different functions and their interactions within the TME can impact tumor initiation and progression. One important type of immune cell found in the TME is tumor-infiltrating lymphocytes (TILs) (4). TILs are a collective term for lymphocytes isolated from tumor tissues, T cells make up the majority, along with other immune cells. Among these, CD8<sup>+</sup> T cells are particularly important as they are responsible for killing tumors and have been associated with improved clinical outcomes (5,6). Recent advancements in immunotherapy have made TIL therapy a promising approach. This involves isolating TILs from a patient's tumor tissue and then stimulating and expanding them in a laboratory setting. The expanded TILs are then reintroduced into the patient to achieve therapeutic goals (7). This approach has shown varying degrees of efficacy in melanoma, cervical cancer, and ovarian cancer (8-10). Compared to traditional chemotherapy, TIL therapy offers better safety as it aims to increase the number of TILs and enhance their killing effect on tumor cells (11). Additionally, these T cells can also regulate tumor cell resistance to drugs and influence the response to chemotherapy (12). Overall, the exploration of the TME and the use of TIL therapy have opened up new possibilities in cancer treatment and provide hope for improved outcomes for patients. With further research and advancements, TIL therapy may become an important component of personalized cancer treatment strategies.

miRNAs, also known as microRNAs, serve as a type of non-coding RNAs that are naturally occurring and have a size of around 22 nucleotides. They govern the levels of gene expression for specific target genes (13). Altered miRNA expression is a frequent occurrence in both cancerous cells and non-tumor elements. miRNAs in tumor cells can serve as either oncogenes and tumor suppressor genes, and some classic ones are already being targeted for anti-tumor therapy (14). In recent years, researchers have increasingly recognized the significance of miRNAs in immune cells that infiltrate tumors. These miRNAs are vital for orchestrating immune control within tumor infiltrations (15). One such miRNA, miR-26a-5p, was found to target tumor cells and inhibit the progression of various carcinomas, including renal cell carcinoma, NSCLC, as well as endometrial cancer (16-18). Yet, the precise regulatory mechanism of miR-26a-5p in tumor-infiltrating T lymphocytes remains unidentified. Further research is needed to understand how this specific miRNA functions in tumor-infiltrating T cells and whether it has any impact on the immune response against cancer cells. Knowing how miR-26a-5p operates to control immune cells within tumor microenvironment could provide valuable insights into developing new therapeutic strategies. Targeting these miRNAs could potentially enhance the anti-tumor immune response and improve the effectiveness of existing immunotherapies. Therefore, more research is warranted to uncover the involvement of miRNAs in immune modulation within tumors as well as their potential for clinical applications in anti-tumor therapy.

The PAM pathway performs a pivotal character in shaping the behavior of cancerous cells, influencing a spectrum of vital functions encompassing growth, viability,

movement, differentiation, and metabolic processes (19). At the core of this cascade, PI3K phosphorylates PIP2 to generate PIP3, which acts as a beckoning signal for oncogenic signaling molecules like AKT (20). This particular protein, renowned for its adeptness in modifying serine and threonine residues, steps in to orchestrate critical cellular responses. The ramifications of Akt's activation extend further as it propels mTOR into action. AKT activates mTOR, which subsequently governs the activity of diverse transcription factors, thereby facilitating the advancement of tumors (21). Interestingly, beyond its direct sway on tumor cells, the intricate PAM signaling pathway exerts a sweeping influence on the activity of T cells that infiltrate the microenvironment of tumors. Evidence underscores the pathway's role in modulating the proliferation and cytotoxic potency of CD8<sup>+</sup>TILs (22). Moreover, this signaling network finely tunes the movement of lymphocytes, impacting their migratory behavior. Pertinently, when PI3K's activity is stymied or its presence is eradicated, the cascade of events that typically propels cytokine-driven lymphocyte infiltration into the tumor microenvironment is arrested (23). The PAM pathway's multifaceted control over cancer cells and the intricate interplay with immune elements like T cells imbue it with a complex role in shaping the tumor landscape.

We employed single-cell sequencing data to conduct a research study focused on examining the miR-26a-5p expression profiles within multiple cellular subpopulations and tissues. Our investigation revealed that miR-26a-5p seems to take part in controlling the activity of T lymphocytes that infiltrate tumors. There has been neither previous report on the regulatory impact of miR-26a-5p, nor its subsequent signaling pathways on CD8<sup>+</sup>TILs in colorectal cancer. Our research's results reveal that miR-26a-5p exerts a negative effect on the PAM signaling pathway's activation through an interaction with EP300, which decreases the activity of lymphocytes that infiltrate tumors and increases the survival of colorectal cancer cells. These discoveries contribute to the progress the creation of an inhibitor linked to miR-26a-5p, which is able to enhance the activity of CD8<sup>+</sup>TILs and improve the therapeutic efficacy of tumor-infiltrating T lymphocyte immunotherapy.

## Materials and Methods

### Target gene of miRNA prediction

For target gene of miR-26a-5p predicted analysis, we perform prediction by miRDB (24), and the threshold of target gene is set to score greater than or equal to 90.

### Differentially expressed gene analysis

Read counts for all genes were normalized using ERgene (25) (v.1.2.0) and DESeq2 (26) (v.1.32.0). Differentially expressed genes were found using the DESeq2 results function (adjusted P-value < 0.05).

### Single-cell RNA sequencing data processing

Cells with fewer than 200 features and more than 25% mitochondrial content were removed for quality control. Features expressed in fewer than 200 cells were also discarded. Data analysis and visualization were conducted using SCANPY v1.4.6 (27). Doublets were identified and removed using Scrublet v0.2.1 (28), based on cluster-based evaluation. Clusters with high scrublet scores in

dimension reduction (such as t-SNE, UMAP) and exhibiting marker gene patterns similar to two or more other clusters were designated as doublets and excluded from subsequent analysis. SCANPY was employed for data analysis and visualization with the following steps: 1. Expression levels were normalized to counts per 10,000 (NC). 2. Log2 transformation:  $\log_2(\text{NC} + 1)$ . 3. Highly variable genes (HVG) were selected based on log-transformed data. 4. Principal component analysis (PCA) was performed using HVGs. If specific cell subsets required analysis, the HVG and PCA steps were repeated. To integrate data from different samples and 10× experiment versions, SCVI (version 0.19.0) (29) was applied to the HVGs for each sample. UMAP and Leiden clustering were performed using SCANPY based on the SCVI-corrected latent space. Data visualization utilized SCANPY and seaborn.

### Cell culture

Mouse colon cancer cell CT26. WT was purchased from Wuhan Procell Life Science & Technology Co., Ltd. (Wuhan, China). The cells containing 10% FBS and 1% penicillin/streptomycin were cultured in RPMI-1640 medium at 37°C in a 5% CO<sub>2</sub> incubator.

### Isolation, culture and activation of CD8<sup>+</sup>TILs

The isolation and culture of TILs were referred to the methods of Li et al. (22) In brief, CT26 cells were inoculated subcutaneously into C57BL/6 mice (Charles River), and after a duration of two weeks, the mice were subjected to cervical dislocation for euthanasia purposes. Subsequently, the tumor nodules located beneath the skin were surgically excised. The tumor tissue was fully cut into 1 mm<sup>3</sup> and digested in RPMI medium containing DNaseI (#07900, Stemcell, Vancouver, Canada) and Collagenase IV (#07909, Stemcell, Vancouver, Canada), filtering with a 70 μm cell strainer. Mouse tumor infiltrating tissue lymphocyte isolation fluid kit (P9000, Solarbio, Beijing, China) was used to extract total TILs. CD8<sup>+</sup>TILs were isolated by EasySep™ Mouse CD8<sup>+</sup> T Cell Isolation Kit (#19853, Stemcell, Vancouver, Canada). The isolated CD8<sup>+</sup> TILs were cultured using RPMI-1640 base medium containing 10% fetal bovine serum and 2 ng/ml mIL-2 (CK24, Novoprotein). The T cell medium contained a mouse CD3/CD28 T cell activator (11456D) during the initial culture.

### Cell viability assay (CCK-8 method).

Cells of the logarithmic growth stage were centrifuged, suspended and counted. Afterward, the cells were introduced into 96-well plates with a density of  $5 \times 10^3$  per well and nurtured using 100 ul of full medium. Following a 24-hour incubation period, 10 microliters of CCK-8 solution were introduced into every well and left to incubate at a temperature of 37 degrees Celsius for a duration of 2 hours. Following incubation, the absorbance at a wavelength of 450 nm was determined using the enzyme label.

### Apoptosis evaluated by flow cytometry.

CT26 cells were inoculated in 6-well plates at a density of  $3 \times 10^5$ / well. After co-culture with tumor-infiltrating lymphocytes for 48 h, Annexin V-FITC/PI Apoptosis Detection Kit (A211-01, Vazyme, Nanjing, China) was used for staining. The percentage of apoptotic cells was measured by flow cytometry. Double-positive cells in the

upper right (Q2) quadrant were defined as late apoptotic cells and analyzed.

### Flow cytometry.

Using LAMP-1 Monoclonal Antibody (eBio1D4B (1D4B)) for CD107a, Alexa Fluor™ 488, eBioscience™ (1:1000; 53-1071-82; Invitrogen, Carlsbad, CA, USA) examined the proportion of CD107a-positive cells in tumor-infiltrating lymphocytes. The data was gathered using the BD LSRFortessa flow cytometer, and the collected data was subsequently analyzed using the FlowJo software.

### ELISA

The Mouse TNF-α ELISA Kit (E-EL-M3063, Elabscience, Wuhan, China) and the Mouse Interferon Gamma (IFN-γ) ELISA Kit (E-EL-M0048c, Elabscience, Wuhan, China) were utilized for the measurement of TNF-α and IFN-γ levels in the culture supernatant of CD8<sup>+</sup>TILs.

### qPCR.

Total microRNAs were isolated using MiPure Cell/Tissue miRNA Kit (RC201, Vazyme, Nanjing, China). miR-26a-5p levels were detected by using the miRNA Universal SYBR qPCR Master Mix (MQ101-01, Vazyme, Nanjing, China) after reverse transcription of the miRNA to cDNA with the miRNA 1st Strand cDNA Synthesis Kit (by tailing A) (MR201-01, Vazyme, Nanjing, China). Detection was performed using the Accurate 96 Real-time fluorescence quantitative PCR System (Accurate 96, DLAB, Beijing, China). The experiment utilized the following primers: U6 (forward primer: 5'- GCTTCGGCAGCACATATAC-TAAAAT-3'; reverse primer: 5'- CGCTTCACGAATT-GCGTGTTCAT'); miR-26a-5p (forward primer: 5'- TT-CAAGTAATCCAGGATAGGCT-3'); and reverse primer: universal primers provided with the kit. The comparative Ct (2-ΔΔCT) method was utilized to calculate the relative gene expression, with genes normalized to U6.

### Western blot.

Cells were disrupted by employing RIPA buffer containing a blend of protease inhibitors and phosphatase inhibitors. Quantification of protein concentrations was performed using the TaKaRa BCA Protein Assay Kit from TaKaRa (Tokyo, Japan) (T9300A). Subsequently, the SDS-PAGE technique was utilized to segregate uniform quantities of total protein, which were then translocated onto PVDF membranes (Millipore, Bedford, MA, USA). To impede nonspecific binding, a solution comprising 5% non-fat milk in Tris-buffered saline was applied for a span of 1 hour. Post this step, primary antibodies were introduced and allowed to incubate at a temperature of 4°C overnight. After a series of washes using TBST, the membranes underwent probing with appropriate secondary antibodies tagged with HRP, and this was followed by an incubation of 2 hours at room temperature. The antibodies that bound were visualized through autoradiography using ECL reagents (180-5001, Tanon, Shanghai, China). The antibodies used in the experiment included Mouse Anti-Gapdh mAb (TA-08; ZSGB-BIO, Beijing, China) at a dilution of 1:2000, mTOR (7C10) Rabbit mAb (#2983; CST, Danvers, MA, USA) at a dilution of 1:1000, Phospho-mTOR (Ser2448) (D9C2) XP® Rabbit mAb (#5536; CST, Danvers, MA, USA) at a dilution of 1:1000, PI3 Kinase p110 Alpha Monoclonal antibody (67071-1-Ig;

proteintech, Rosemont, IL, USA) at a dilution of 1:1000, RabbitAnti-phospho-PI3KCA (Tyr317) antibody (bs-5570R; Bioss, Woburn, MA, USA) at a dilution of 1:500, AKT Monoclonal antibody (60203-2-Ig; proteintech, Rosemont, IL, USA) at a dilution of 1:1000, Phospho-AKT (Ser473) Monoclonal antibody (66444-1-Ig; proteintech, Rosemont, IL, USA) at a dilution of 1:500, Anti-KAT3B / p300 antibody (EPR23495-268) - ChIP Grade (ab275378; abcam, Cambridge, MA, USA) at a dilution of 1:1000, Caspase-9 Antibody (#9504; CST, Danvers, MA, USA) at a dilution of 1:500, Caspase 3/p17/p19 Polyclonal antibody (19677-1-AP; proteintech, Rosemont, IL, USA) at a dilution of 1:500, Bcl2 Monoclonal antibody (68103-1-Ig; proteintech, Rosemont, IL, USA) at a dilution of 1:500, BAX Polyclonal antibody (50599-2-Ig; proteintech, Rosemont, IL, USA) at a dilution of 1:500, HRP, Goat Anti-Rabbit IgG (A21020; Abbkine, Wuhan, China) at a dilution of 1:10000, and HRP, Goat Anti-Mouse IgG (A21010; Abbkine, Wuhan, China) at a dilution of 1:10000.

### Lactate Dehydrogenase (LDH) Assay.

The LDH cytotoxicity assay kit (C0016, Beyotime, Shanghai, China) was used to evaluate cell death. After 48 hours of co-culturing CT26 cells with CD8<sup>+</sup>TILs, the resulting culture supernatants were transferred to a 96-well plate. Furthermore, all cells were lysed at the highest absorbance, while the absorbance of the culture medium served as the control. Afterward, the mixture of chemicals was introduced into a 96-well plate and left to incubate for 30 minutes at ambient temperature. Following the addition of the stop solution, the spectrophotometer was used to measure the OD values at 490 nm and 600 nm. The calculation of cell death ratio was performed by applying the subsequent equation: Cell death percentage equals (Absorbance sample minus Absorbance control) divided by (Absorbance maximum minus Absorbance control), multiplied by 100.

### Experiments using the Dual-Luciferase Reporter Assays.

To confirm the interaction of miR-26a-5p with its possible target gene EP300. Lipofectamine 3000 (L3000075, Invitrogen, Carlsbad, CA, USA) was employed for the co-transfection of miR-26a-5p mimics and EP300 wild-type and mutant plasmid. After a 48-hour period, the Dual-Luciferase Reporter Assay System from Promega located in Maddison, WI, WI was utilized. USA) Detect the Renilla luciferase and firefly luciferase activities. Firefly luciferase activity was normalized using Renilla luciferase activity as an internal control. MiaoLingBio, a company based in China, synthesized the reporter genes with EP300-WT and EP300-Mut.

### Cell Transfection with miRNA mimic and inhibitor.

$2 \times 10^5$  cells in the logarithmic growth phase were added to each well of 6-well plates. The micrON mmu-miR-26a-5p mimic (miR10000533-1-5, RIBOBIO, Guangzhou, China) was transfected overnight with the riboFECT CP Transfection Kit (C10511-05, RIBOBIO, Guangzhou, China). The cells were transfected with micrOFF mmu-miR-26a-5p inhibitor (miR20000533-1-5, RIBOBIO, Guangzhou, China) and negative controls (NC) (RIBOBIO, Guangzhou, China) at a transfection reagent concentration of 25 nM.

### Gene Knockdown

The plasmid pLV3-U6-Ep300(mouse)-shRNA1-CopGFP-Puro(P47732) was acquired from MiaoLingBio in China. The manufacturer's instruction was followed to package recombinant lentiviruses. Cultivated cells were exposed to lentiviral fluids containing 8  $\mu\text{g}/\text{mL}$  polybrene for a duration of 24 hours. Following this, a new solution was introduced into the medium, which was then incubated for an extra 48 hours. Cells were chosen for stable cell line generation using a puromycin concentration of 3  $\mu\text{g}/\text{mL}$ .

### Statistical analysis

The data were presented as mean  $\pm$  SD and were analyzed using Statistic Package for Social Science (SPSS) 22.0 (IBM, Armonk, NY, USA) and GraphPad Prism 8.0 software (La Jolla, CA, USA). To examine the disparity between the two groups, the t-test was conducted. Data from three separate experiments were collected. A P-value below 0.05 was deemed statistically significant.

### Results

#### Expression of miR-26a-5p in different anatomical sites and cells.

We obtained samples of human colorectal cancer core, cancer margin, para-cancerous tissue, and normal human colon tissue from public databases. After conducting quality assurance (Figure 1A, 1B), we acquired a grand total of 81,605 cells, comprising 39,437 cells from healthy tissue, 15,241 cells from tumor cores, 13,428 cells from tumor margins, and 13,499 cells from paracancerous tis-

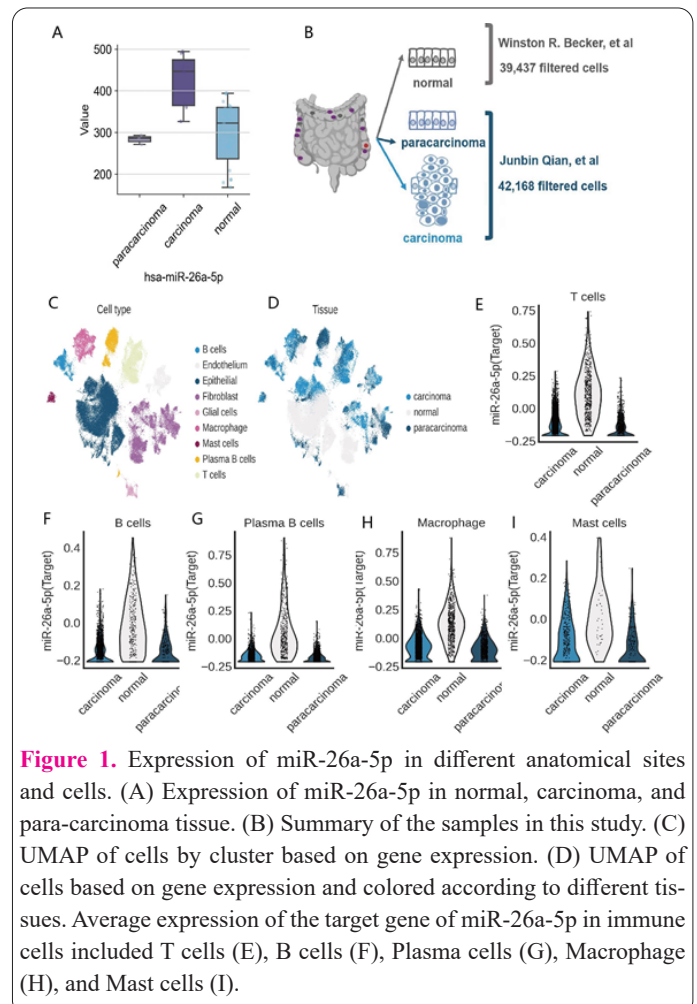


**Figure 1.** Expression of miR-26a-5p in different anatomical sites and cells. (A) Expression of miR-26a-5p in normal, carcinoma, and para-carcinoma tissue. (B) Summary of the samples in this study. (C) UMAP of cells by cluster based on gene expression. (D) UMAP of cells based on gene expression and colored according to different tissues. Average expression of the target gene of miR-26a-5p in immune cells included T cells (E), B cells (F), Plasma cells (G), Macrophage (H), and Mast cells (I).

sue. By utilizing established genes that serve as markers for specific cell types (Figure 1C, 1D), we successfully carried out the annotation of cell types. For the purpose of examining how miR-26a-5p impacts on tumor-infiltrating lymphocytes, we calculated the average expression of target genes interacting with miR-26a-5p in each cell and contrasted the target gene's expression across diverse immune cells (Figure 1E-I). In cancer cells, the average expression levels of genes influenced by miR-26a-5p consistently appear to be lower than those observed in T cells, B cells, plasma cells, macrophages, and mast cells.

### The function of CD8<sup>+</sup>TILs is restrained by miR-26a-5p.

We transfected CD8<sup>+</sup>TILs with synthetic miR-26a-5p mimics to validate whether miR-26a-5p takes part in regulating CD8<sup>+</sup>TILs' activity. According to Figure 2A, the qPCR findings revealed an increase in the expression of miR-26a-5p in CD8<sup>+</sup>TILs from the mimics cohorts. Nevertheless, an unchanged result was observed in control cohorts. This outcome implies that miR-26a-5p mimics perhaps can augment the presence of miR-26a-5p in CD8<sup>+</sup>TILs. Subsequently, we examined how miR-26a-5p affected the survival of CD8<sup>+</sup>TILs. According to the findings in Figure 2B, in the CCK-8 experiment, it was observed that the cohorts of miR-26a-5p mimics exhibited a reduced viability of CD8<sup>+</sup>TILs in comparison to both the Control and NC cohorts. Furthermore, we investigated how miR-26a-5p influences the level of CD107a observed in CD8<sup>+</sup>TILs. According to the data presented in Figure 2C, The findings from flow cytometry revealed that the miR-26a-5p mimics cohorts exhibited a decrease in CD107a expression within CD8<sup>+</sup>TILs, in contrast to both the Control and NC cohorts.

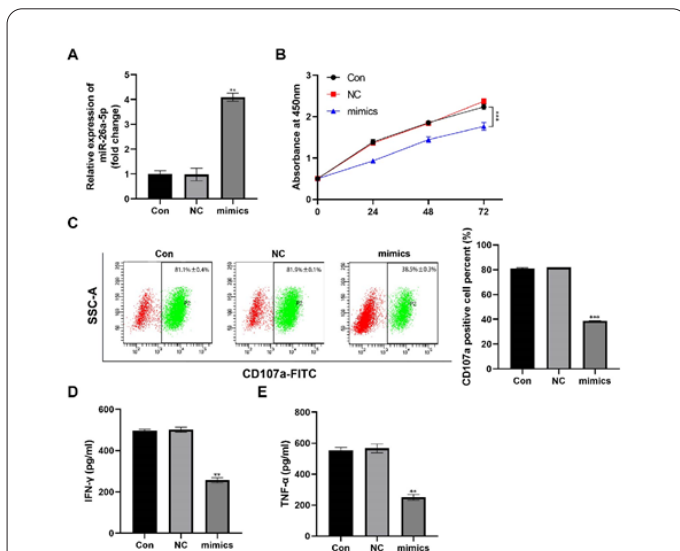


**Figure 2.** The function of CD8<sup>+</sup>TILs is restrained by miR-26a-5p. (A) Following the introduction of miR-26a-5p mimics or miR-26a-5p negative control, CD8<sup>+</sup>TILs underwent qPCR assessment after 48 hours of transfection. (B) The cell viability of CD8<sup>+</sup>TILs in the control, NC, and mimics cohorts was determined through the employment of CCK-8 assay. (C) The expression levels of CD107a in CD8<sup>+</sup>TILs in the control, NC, and mimics cohorts were determined through the employment of flow cytometry. (D, E)ELISA was employed to identify the quantities of IFN- $\gamma$  and TNF- $\alpha$  present in the supernatant of the CD8<sup>+</sup>TILs culture medium in the control, NC, and mimics cohorts. \* for  $P < 0.05$ , \*\* for  $P < 0.01$ , and \*\*\* for  $P < 0.001$ .

To further investigate how miR-26a-5p affects the cytotoxicity of CD8<sup>+</sup>TILs, we evaluated its influence on the quantity of IFN- $\gamma$  and TNF- $\alpha$  within CD8<sup>+</sup>TILs. The outcome of the ELISA experiment, as illustrated in Figures 2D and E, demonstrate the presence of cytokines levels in both the Control and NC cohorts. These outcomes propose that miR-26a-5p hinders the functionality of CD8<sup>+</sup>TILs.

### miR-26a-5p suppressed the PAM signaling pathway's functional involvement in CD8<sup>+</sup>TILs.

To investigate how miR-26a-5p influences the behavior of CD8<sup>+</sup>TILs, we transfected miR-26a-5p mimics and inhibitors to CD8<sup>+</sup>TILs. As shown in Figure 3, Western blot results discovered that miR-26a-5p mimics restrained the expression levels of phosphorylation of PI3K, AKT, and mTOR proteins in CD8<sup>+</sup>TILs, while not affecting their overall abundance. Conversely, the miR-26a-5p inhibitor enhanced the quantities of phosphorylated PI3K, AKT, and mTOR proteins in CD8<sup>+</sup>TILs, with no influence on the total protein levels. Our discoveries imply a connection between the abundance of miR-26a-5p and the functioning of the PAM signaling pathway in CD8<sup>+</sup>TILs. miR-26a-5p restrains the activity of the PAM signaling pathway in CD8<sup>+</sup>TILs.

### EP300 is the target of miR-26a-5p.

Resources were provided by the TargetScan database (<http://www.targetscan.org/>) and the miRDB database (<http://mirdb.org/>), an analysis was conducted to investigate the binding mechanism between miR-26a-5p and EP300, as depicted in Figure 4A. By utilizing a dual-luciferase reporter gene assay, the confirmation of the direct binding between miR-26a-5p and the 3'UTR of EP300 was established. This result is visually represented in Figure 4B. The findings showed that when miR-26a-5p mimics were introduced, there was a decrease in luciferase activity in 293T cells. These cells had been transfected with a plasmid that carried the wild-type EP300 3'UTR sequence. However, when a plasmid containing a mutant EP300 3'UTR was transfected, the luciferase activity of 293T cells remained unaffected.

### miR-26a-5p influences the functionality of the PAM signaling pathway within CD8<sup>+</sup>TILs by targeting EP300.

To validate whether miR-26a-5p modulates the functionality of the PAM signaling pathway in CD8<sup>+</sup>TILs present within tumor tissues, by directly influencing EP300, we performed co-transfections of a miR-26a-5p inhibitor

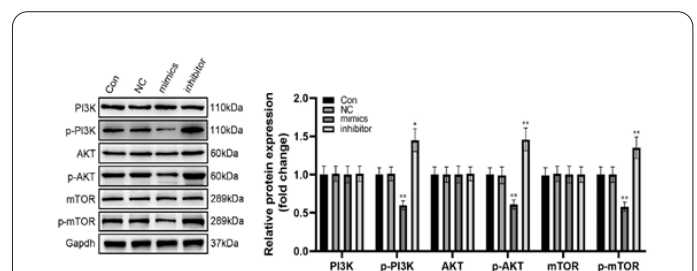
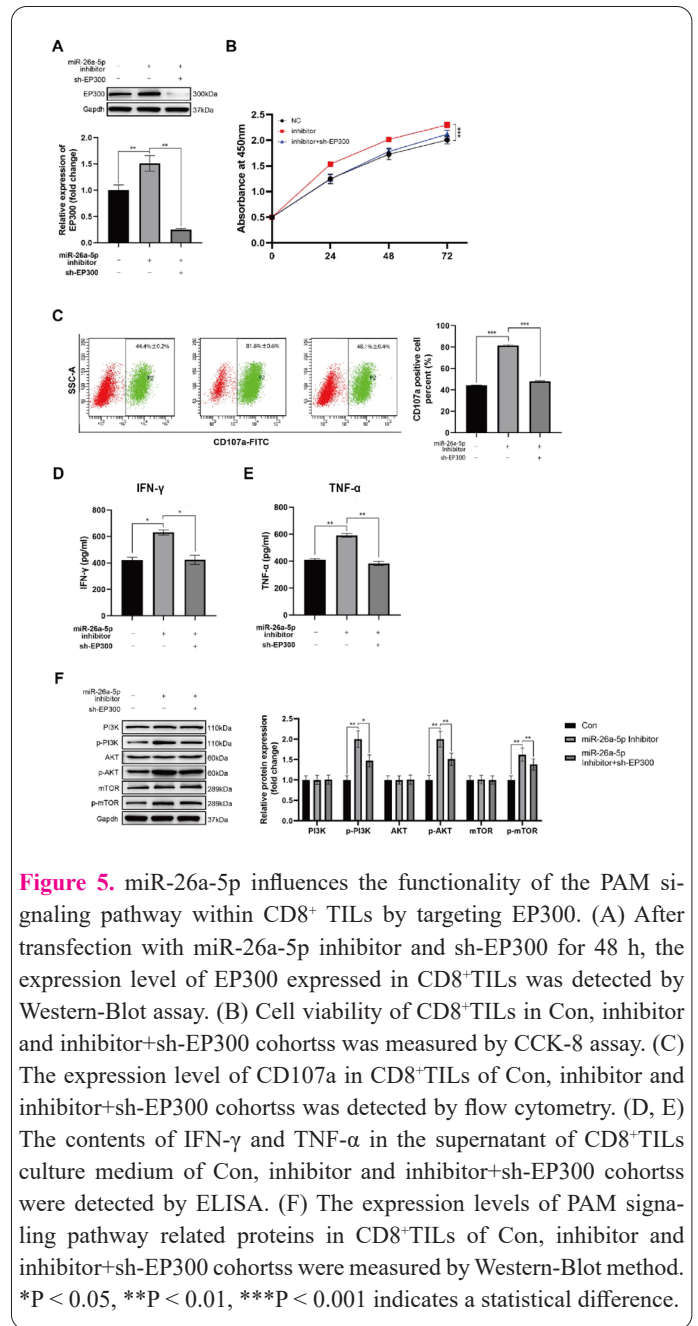
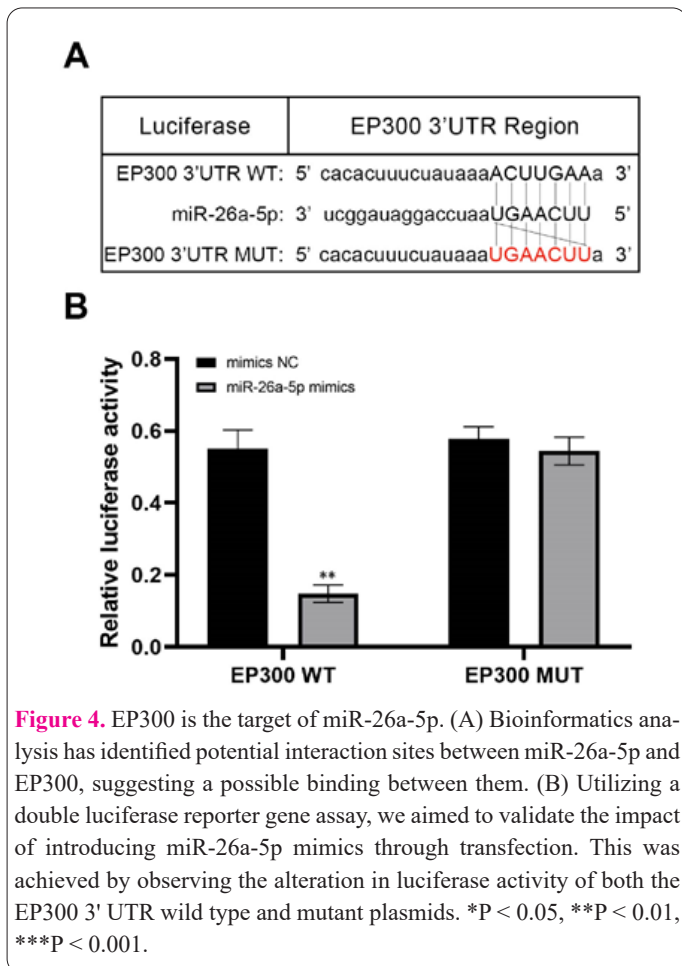


**Figure 3.** miR-26a-5p suppressed the PAM signaling pathway's functional involvement in CD8<sup>+</sup>TILs. The Western Blot technique was employed to identify the presence of proteins linked to the PAM pathway in the Con, NC, mimics, and inhibitor cohorts. \* $P < 0.05$ , \*\* $P < 0.01$ , and \*\*\* $P < 0.001$ .

and a plasmid carrying EP300-specific shRNA in CD8<sup>+</sup> T lymphocytes isolated from tumor-infiltrated regions. Subsequently, we evaluated whether introducing sh-EP300 through transfection could reverse the impact caused by inhibition of miR-26a-5p. According to findings in Figure 5A, the Western Blot data demonstrated that suppressing miR-26a-5p triggered an elevation in the protein levels of EP300 within CD8<sup>+</sup>TILs. Conversely, the suppressive influence of sh-EP300 nullified the upregulatory outcome caused by the miR-26a-5p inhibitor on the levels of EP300 protein. Figure 5B illustrates that the presence of sh-EP300 has the ability to counteract the augmented influence caused by the miR-26a-5p inhibitor on the viability of CD8<sup>+</sup>TILs. Additionally, Figure 5C reveals that sh-EP300 can counteract the promotive influence of the miR-26a-5p inhibitor on the levels of CD107a observed in CD8<sup>+</sup>TILs. The ELISA method was utilized to determine the IFN- $\gamma$  and TNF- $\alpha$  levels in the supernatant of the CD8<sup>+</sup>TILs culture medium. As depicted in Figure 5D, the presence of the miR-26a-5p inhibitor led to elevated levels of IFN- $\gamma$  and TNF- $\alpha$  in the culture supernatant, whereas EP-300 could counteract its promotive effect. Finally, the Western Blot technique was utilized to examine the proteins variations pertaining to the PAM signaling pathway in CD8<sup>+</sup>TILs. The miR-26a-5p inhibitor exhibited an augmenting effect on the levels of p-PI3K, P-AKT, and p-mTOR proteins, as depicted in Figure 5E, resembling the previous section. The levels of p-PI3K, P-AKT, and p-mTOR proteins showed a reduction in response to Sh-EP300 when the miR-26a-5p inhibitor was present. Our findings suggest that miR-26a-5p directly target EP300, leading to the modulation of CD8<sup>+</sup>TILs. Additionally, this



interaction has an impact on the regulatory condition of the PAM signaling pathway.

**miR-26a-5p targets EP300 to inhibit the activity of CD8<sup>+</sup>TILs and promote the survival of colon cancer cells.**

To confirm whether miR-26a-5p regulates CD8<sup>+</sup>TILs by targeting EP300 and impacts tumor cell survival, we simultaneously introduced miR-26a-5p inhibitor and EP300-specific shRNA plasmid into CD8<sup>+</sup>TILs. Subsequently, we co-cultured these cells with CT26 cells. We investigated the transfection of sh-EP300 to assess if it could negate the cytotoxicity of CD8<sup>+</sup>TILs by enhancing the impact of miR-26a-5p inhibitor. According to the data shown in Figure 6A, the LDH detection results indicated that the volume of LDH secretion by CT26 cells increased in the co-cultured system with CD8<sup>+</sup>TILs, in contrast to the control cohort of CT26 cells. In the TILs co-culture system, the LDH levels of CT26 cells were further enhanced by inhibiting miR-26a-5p. However, the increase

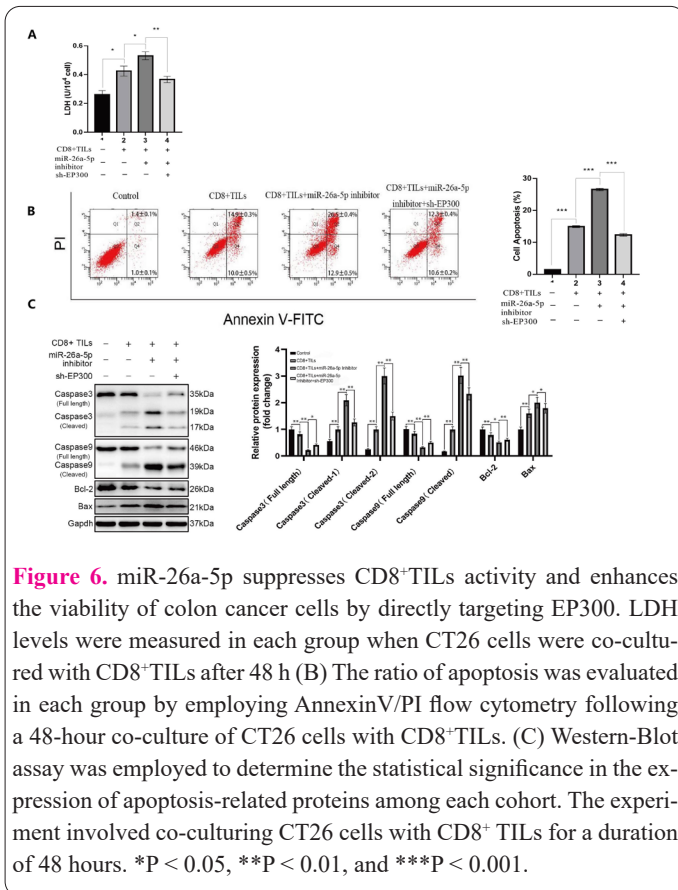


**Figure 6.** miR-26a-5p suppresses CD8<sup>+</sup>TILs activity and enhances the viability of colon cancer cells by directly targeting EP300. LDH levels were measured in each group when CT26 cells were co-cultured with CD8<sup>+</sup>TILs after 48 h (B) The ratio of apoptosis was evaluated in each group by employing AnnexinV/PI flow cytometry following a 48-hour co-culture of CT26 cells with CD8<sup>+</sup>TILs. (C) Western-Blot assay was employed to determine the statistical significance in the expression of apoptosis-related proteins among each cohort. The experiment involved co-culturing CT26 cells with CD8<sup>+</sup>TILs for a duration of 48 hours. \*P < 0.05, \*\*P < 0.01, and \*\*\*P < 0.001.

in LDH levels of CT26 cells caused by miR-26a-5p inhibitor existed in TILs co-culture system was counteracted by sh-EP300. According to the findings in Figure 6B, Flow cytometry data showed that the co-cultured TILs system increased the apoptosis rate of CT26 cells in contrast to the CT26 cell control cohorts. Inhibition of miR-26a-5p further facilitate the apoptosis rate of CT26 cells in the TILs co-culture system, while sh-EP300 could counteract the increase in apoptosis ratio of CT26 cells induced by miR-26a-5p inhibitor in the TILs co-culture system. Figure 6C showed that the TILs co-culture system significantly led to elevated levels of pro-apoptotic proteins (Cleaved-Caspase3, Cleaved-Caspase9, and Bax) and decreased levels of apoptosis suppressor protein (Bcl-2) in CT26 cells, in comparison to the control cohorts CT26 cells. The miR-26a-5p inhibitor resulted in a greater expression of apoptosis-related proteins. However, the introduction of sh-EP300 was able to reverse the alteration in the expression of these proteins caused by the miR-26a-5p inhibitor in the co-culture system of CT26 cells.

## Discussion

Surgical removal remains the primary and foundational approach for the treatment of colorectal cancer. This often involves resecting the affected portion of the colon or rectum to remove the cancerous tissue. However, the management of colorectal cancer typically involves a multidisciplinary approach, which may include the supplementary use of chemotherapy and radiation therapy. Chemotherapy is employed to target cancer cells throughout the body. It utilizes drugs that circulate through the bloodstream, reaching cancer cells even when they have spread beyond the primary tumor site. Radiation therapy, on the other hand, employs high-energy beams to target and destroy

cancer cells. It is often used after surgery to eliminate any remaining cancer cells or as a palliative measure to relieve symptoms in advanced cases. While surgical and traditional treatment methods have been effective, there is growing optimism surrounding immunotherapy as an additional and promising approach. Immunotherapy distinguishes itself from conventional treatments by leveraging the innate defense mechanism of the organism to counteract cancer. This approach offers several advantages, notably the potential to minimize the adverse effects on normal cells caused by conventional tumor treatments. Tumor immunotherapy has shown significant promise in preventing cancer metastasis and reducing the risk of recurrence (30). Key to its success is the presence of Cytotoxic Lymphocytes within the TME. They have a pivotal function in mounting an immune reaction targeting the tumor (31). CD8<sup>+</sup>TILs are known for their cytotoxicity, meaning they have the ability to directly kill malignant tumor cells. Their proper function is crucial in impeding the progression of tumor malignancy. Conversely, when CD8<sup>+</sup>TILs become dysfunctional or depleted, it can exacerbate the aggressiveness of the tumor (32). While surgical removal remains the primary treatment approach for colorectal cancer, the integration of chemotherapy and radiation therapy is common practice. Immunotherapy presents a promising advancement in cancer treatment by leveraging the body's immune system to combat tumors while minimizing collateral damage to healthy cells. The presence and functionality of CD8<sup>+</sup>TILs within the tumor microenvironment are pivotal in orchestrating an effective immune response against colorectal cancer, ultimately contributing to better outcomes and reduced risk of metastasis and recurrence.

MicroRNAs (miRNAs) are pivotal in post-transcriptional gene regulation, particularly in the context of immune cells within the tumor microenvironment (TME). In our preliminary investigations, We uncovered a robust correlation linking miR-26a-5p with the function of infiltrating T lymphocytes within tumors. Employing a combination of bioinformatics predictions and experimental validation, we confirmed the significant role of EP300 in governing CD8<sup>+</sup> tumor-infiltrating T lymphocyte activity through miR-26a-5p. This highlights a recurring theme wherein miRNAs serve as potential mechanisms for tumor cells to evade immune surveillance by modulating immune cell activity. Additionally, we observed that reduced miR-34a levels in the TME lead to increased LDHA expression and lactate accumulation. This, in turn, diminishes T lymphocyte infiltration, enabling gastric cancer cells to evade immune suppression effectively (33). Conversely, heightened expression of miR-155 enhances the cytotoxicity of CD8<sup>+</sup> tumor-infiltrating lymphocytes in melanoma (34), while elevated levels of miR-34a-5p or miR-22-3p inhibit the activity of these lymphocytes (35). This parallels our findings with miR-26a-5p, indicating that dysregulated miRNA expression profoundly influences the behavior of tumor-infiltrating T lymphocytes within the TME. However, it's crucial to note that our investigation couldn't pinpoint the exact source of miR-26a-5p within the TME. This unresolved mystery will be a primary focus for future studies in our quest to comprehensively understand the intricate regulatory network of miRNAs in the TME and their impact on immune cell dynamics. Uncovering the origin of miR-26a-5p will undoubtedly shed more light on the complex interplay between miRNAs, immune cells,

and tumor cells.

In cellular environments, the intricate interplay between EP300 and miR-26a-5p has been unveiled, substantiated by dual luciferase reporter gene assays. These interactions contribute to a dynamic regulatory network. As pivotal transcriptional coactivators, EP300 and CBP govern histone acetylation through their Histone Acetyltransferase (HAT) activity, wielding profound influence over transcriptional regulation while displaying high conservation (36,37). This process involves the acetyl groups being transferred to the  $\epsilon$ -amino units found within histone lysine residues, fostering heightened histone acetylation levels and thereby fostering the expression of a plethora of genes (38). The role played by EP300 within the Tumor Microenvironment (TME) is remarkably dualistic. On one facet, an excess of EP300 potentially expedites cancer cell initiation and progression. Noteworthy reports delineate how the NF- $\kappa$ B/EP300 signaling pathway is set into motion by CXCL1, thereby underpinning the advancement of colon cancer (39). Conversely, quelling EP300 activity expedites NF- $\kappa$ B-triggered Foxp3 expression, impeding the generation of TGF- $\beta$ -induced Tregs. This inhibition effectively diminishes the Foxp3 Tregs subset amidst tumor-infiltrating lymphocytes, consequently heightening cytotoxicity against tumors (40).

The intricate interplay between EP300 and the PAM pathway was illuminated through comprehensive investigations, including a notable recovery experiment. This experiment aptly showcases that EP300 plays a pivotal role in modulating the PAM pathway for its initiation. This finding harmonizes seamlessly with previous scholarly reports which affirm that EP300 exerts its influence by orchestrating the elevation of H3K27ac levels, thereby propelling the excitation of the PAM axis (41). Furthermore, intriguing insights have emerged from specific studies that highlight a reciprocal relationship. Notably, the PAM pathway assumes a commanding role in dictating the expression levels of EP300. Through intricate mechanisms, this pathway fosters heightened activation, thereby providing impetus to the augmentation of EP300 expression. This orchestrated activation of EP300 subsequently cascades into the transactivation of the SOX9 gene transcription. Remarkably, this molecular symphony takes center stage in the intricate regulation of phenotype within intervertebral disc nucleus cells (42). Yet, it is important to underscore that the interaction between EP300 and the PAM signaling pathway defies a simplistic cascade model. This nexus between EP300 and the PAM axis is poised to be more intricate and nuanced, thus necessitating a deeper plunge into comprehensive research endeavors. The contours of this intricate crosstalk demand further probing to unravel the complex regulatory dance that underlies the interplay between EP300 and multifaceted PAM pathway. In essence, the fascinating relationship beckons for a deeper understanding, shedding light on the orchestration of molecular mechanisms that govern cellular phenotypic regulation.

## Conclusions

In this study, we explored the function and underlying molecular mechanisms of miR-26a-5p concerning the behavior of CD8<sup>+</sup>TILs. The empirical outcomes indicate that miR-26a-5p hinders the operation of CD8<sup>+</sup>TILs by reducing the extent of activation within the PAM signaling pa-

thway. EP300 was pinpointed as a downstream target gene affected by miR-26a-5p. Suppression of EP300 countered the heightened operation of CD8<sup>+</sup>TILs triggered by the introduction of the miR-26a-5p inhibitor. Furthermore, EP300 facilitated the control exerted by miR-26a-5p over the degree of activation in the PAM signaling pathway. Diminishing EP300 presence mitigated the escalated activation of the PAM signaling pathway caused by the miR-26a-5p inhibitor. These empirical findings contribute to an improved comprehension of how alterations in miRNA levels impact TME. The strategic targeting of miRNAs could potentially amplify the effectiveness of immune therapy utilizing CD8<sup>+</sup>TILs for treating tumors.

## Author Contributions

Conceptualization, C.W. and CM.W.; methodology, C.W., YX.L. and HN.L.; software, C.W., HN.L., Y.C.; validation, C.W., HN.L. and Y.C.; formal analysis, C.W. WQ.Z. and YX.L; investigation, C.W., HN.L. and WQ.Z; resources, CM.W.; data curation, C.W.; writing—original draft preparation, C.W.; writing—review and editing, C.W. and CM.W.; visualization, C.W.; supervision, CM.W.; project administration, CM.W.; funding acquisition, none. All authors have read and agreed to the published version of the manuscript.

## Funding

This research received no external funding

## Institutional Review Board Statement

The animal study protocol was approved by the Ethics Committee for Animal Experiment of Dalian Medical University (protocol code AEE21065, approval date: 2021.12.6).

## Data Availability Statement

The previously published miRNA data of para-carcinoma and carcinoma are available under accession codes GSE183437, and healthy colon and CRC sample are available under accession codes GSE160432. Previously published scRNA-seq of healthy colon data are available under accession codes GSE201349, para-carcinoma and carcinoma are available in <https://www.ebi.ac.uk/biostudies/arrayexpress/studies/E-MTAB-8107/sdrf>

## Code Availability Statement

The analysis code can be found in <https://zenodo.org/doi/10.5281/zenodo.8275935>

## Acknowledgments

None.

## Conflicts of Interest

The authors declare no conflict of interest.

## References

1. Siegel RL, Miller KD, Fuchs HE, Jemal A. Cancer statistics, 2022. *Ca-Cancer J Clin* 2022; 72(1): 7-33.
2. Miller KD, Nogueira L, Devasia T, et al. Cancer treatment and survivorship statistics, 2022. *Ca-Cancer J Clin* 2022; 72(5): 409-436.
3. Wang L, Yang G, Liu G, Pan Y. Identification of lncRNA Signature of Tumor-Infiltrating T Lymphocytes With Potential Implica-

- tions for Prognosis and Chemotherapy of Head and Neck Squamous Cell Carcinoma. *Front Pharmacol* 2021; 12: 795205.
4. Yue Y, Zhang Q, Sun Z. CX3CR1 Acts as a Protective Biomarker in the Tumor Microenvironment of Colorectal Cancer. *Front Immunol* 2021; 12(758040).
  5. Nelson MA, Ngamcherdrakul W, Luoh SW, Yantasee W. Prognostic and therapeutic role of tumor-infiltrating lymphocyte subtypes in breast cancer. *Cancer Metast Rev* 2021; 40(2): 519-536.
  6. Kiessler M, Plesca I, Sommer U, et al. Tumor-infiltrating plasmacytoid dendritic cells are associated with survival in human colon cancer. *J Immunother Cancer* 2021; 9(3):
  7. Albrecht HC, Gustavus D, Schwanemann J, et al. Generation of colon cancer-derived tumor-infiltrating T cells (TILs) for adoptive cell therapy. *Cytotherapy* 2023; 25(5): 537-547.
  8. Rosenberg SA, Yang JC, Sherry RM, et al. Durable complete responses in heavily pretreated patients with metastatic melanoma using T-cell transfer immunotherapy. *Clin Cancer Res* 2011; 17(13): 4550-4557.
  9. Oberg HH, Janitschke L, Sulaj V, et al. Bispecific antibodies enhance tumor-infiltrating T cell cytotoxicity against autologous HER-2-expressing high-grade ovarian tumors. *J Leukocyte Biol* 2020; 107(6): 1081-1095.
  10. Stevanovic S, Draper LM, Langhan MM, et al. Complete regression of metastatic cervical cancer after treatment with human papillomavirus-targeted tumor-infiltrating T cells. *J Clin Oncol* 2015; 33(14): 1543-1550.
  11. Aparicio C, Belver M, Enriquez L, et al. Cell Therapy for Colorectal Cancer: The Promise of Chimeric Antigen Receptor (CAR)-T Cells. *Int J Mol Sci* 2021; 22(21):
  12. Zarogoulidis P, Petanidis S, Domvri K, et al. Autophagy inhibition upregulates CD4(+) tumor infiltrating lymphocyte expression via miR-155 regulation and TRAIL activation. *Mol Oncol* 2016; 10(10): 1516-1531.
  13. Xu Y, Liu Z, Lv L, et al. MiRNA-340-5p mediates the functional and infiltrative promotion of tumor-infiltrating CD8(+) T lymphocytes in human diffuse large B cell lymphoma. *J Exp Clin Canc Res* 2020; 39(1): 238.
  14. Jiang M, Yang Y, Niu L, et al. MiR-125b-5p modulates the function of regulatory T cells in tumor microenvironment by targeting TNFR2. *J Immunother Cancer* 2022; 10(11):
  15. Yang J, Liu R, Deng Y, et al. MiR-15a/16 deficiency enhances anti-tumor immunity of glioma-infiltrating CD8+ T cells through targeting mTOR. *Int J Cancer* 2017; 141(10): 2082-2092.
  16. Wang XJ, Chen L, Xu R, Li S, Luo GC. DLEU7-AS1 promotes renal cell cancer by silencing the miR-26a-5p/coronin-3 axis. *Clin Kidney J* 2022; 15(8): 1542-1552.
  17. Wang RQ, Long XR, Zhou NN, et al. Lnc-GAN1 expression is associated with good survival and suppresses tumor progression by sponging mir-26a-5p to activate PTEN signaling in non-small cell lung cancer. *J Exp Clin Canc Res* 2021; 40(1): 9.
  18. Liu Y, Cai Y, Chang Y. Dual inhibition of RNAi therapeutic miR-26a-5p targeting cMet and immunotherapy against EGFR in endometrial cancer treatment. *Ann Transl Med* 2021; 9(1): 5.
  19. Fruman DA, Chiu H, Hopkins BD, Bagrodia S, Cantley LC, Abraham RT. The PI3K Pathway in Human Disease. *Cell* 2017; 170(4): 605-635.
  20. Vanhaesebroeck B, Guillermet-Guibert J, Graupera M, Bilanges B. The emerging mechanisms of isoform-specific PI3K signaling. *Nat Rev Mol Cell Bio* 2010; 11(5): 329-341.
  21. Yu L, Wei J, Liu P. Attacking the PI3K/Akt/mTOR signaling pathway for targeted therapeutic treatment in human cancer. *Semin Cancer Biol* 2022; 85: 69-94.
  22. Li P, Zhou D, Chen D, et al. Tumor-secreted IFI35 promotes proliferation and cytotoxic activity of CD8(+) T cells through PI3K/AKT/mTOR signaling pathway in colorectal cancer. *J Biomed Sci* 2023; 30(1): 47.
  23. Chandrasekaran S, Funk CR, Kleber T, Paulos CM, Shanmugam M, Waller EK. Strategies to Overcome Failures in T-Cell Immunotherapies by Targeting PI3K-delta and -gamma. *Front Immunol* 2021; 12: 718621.
  24. Chen Y, Wang X. miRDB: an online database for prediction of functional microRNA targets. *Nucleic Acids Res* 2020; 48(D1): D127-D131.
  25. Zeng Z, Xiong Y, Guo W, Du H. ERgene: Python library for screening endogenous reference genes. *Sci Rep-Uk* 2020; 10(1): 18557.
  26. Love MI, Huber W, Anders S. Moderated estimation of fold change and dispersion for RNA-seq data with DESeq2. *Genome Biol* 2014; 15(12): 550.
  27. Wolf FA, Angerer P, Theis FJ. SCANPY: large-scale single-cell gene expression data analysis. *Genome Biol* 2018; 19(1): 15.
  28. Wolock SL, Lopez R, Klein AM. Scrublet: Computational Identification of Cell Doublets in Single-Cell Transcriptomic Data. *Cell Syst* 2019; 8(4): 281-291.
  29. Gayoso A, Lopez R, Xing G, et al. A Python library for probabilistic analysis of single-cell omics data. *Nat Biotechnol* 2022; 40(2): 163-166.
  30. Fabregas JC, Ramnarain B, George TJ. Clinical Updates for Colon Cancer Care in 2022. *Clin Colorectal Canc* 2022; 21(3): 198-203.
  31. Rooney MS, Shukla SA, Wu CJ, Getz G, Hacohen N. Molecular and genetic properties of tumors associated with local immune cytolytic activity. *Cell* 2015; 160(1-2): 48-61.
  32. Zhu J, Yan M, Yan H, et al. Single-Cell Transcriptomic Analysis Reveals the Crosstalk Propensity Between the Tumor Intermediate State and the CD8+ T Exhausted State to be Associated with Clinical Benefits in Melanoma. *Front Immunol* 2022; 13: 766852.
  33. Ping W, Senyan H, Li G, Yan C, Long L. Increased Lactate in Gastric Cancer Tumor-Infiltrating Lymphocytes Is Related to Impaired T Cell Function Due to miR-34a Deregulated Lactate Dehydrogenase A. *Cell Physiol Biochem* 2018; 49(2): 828-836.
  34. Martinez-Usatorre A, Sempere LF, Carmona SJ, et al. MicroRNA-155 Expression Is Enhanced by T-cell Receptor Stimulation Strength and Correlates with Improved Tumor Control in Melanoma. *Cancer Immunol Res* 2019; 7(6): 1013-1024.
  35. Galore-Haskel G, Greenberg E, Yahav I, et al. microRNA expression patterns in tumor infiltrating lymphocytes are strongly associated with response to adoptive cell transfer therapy. *Cancer Immunol Immun* 2021; 70(6): 1541-1555.
  36. Goodman RH, Smolik S. CBP/p300 in cell growth, transformation, and development. *Gene Dev* 2000; 14(13): 1553-1577.
  37. Chan HM, La Thangue NB. p300/CBP proteins: HATs for transcriptional bridges and scaffolds. *J Cell Sci* 2001; 114(Pt 13): 2363-2373.
  38. Henry RA, Kuo YM, Andrews AJ. Differences in specificity and selectivity between CBP and p300 acetylation of histone H3 and H3/H4. *Biochemistry-U S* 2013; 52(34): 5746-5759.
  39. Zhuo C, Ruan Q, Zhao X, Shen Y, Lin R. CXCL1 promotes colon cancer progression through activation of NF-kappaB/P300 signaling pathway. *Biol Direct* 2022; 17(1): 34.
  40. MaruYama T, Kobayashi S, Nakatsukasa H, et al. The Curcumin Analog GO-Y030 Controls the Generation and Stability of Regulatory T Cells. *Front Immunol* 2021; 12: 687669.
  41. Wei D, Rui B, Qingquan F, et al. KIF11 promotes cell proliferation via ERBB2/PI3K/AKT signaling pathway in gallbladder cancer. *Int J Biol Sci* 2021; 17(2): 514-526.
  42. Cheng CC, Uchiyama Y, Hiyama A, Gajghate S, Shapiro IM, Ribud MV. PI3K/AKT regulates aggrecan gene expression by mo-

dulating Sox9 expression and activity in nucleus pulposus cells

of the intervertebral disc. *J Cell Physiol* 2009; 221(3): 668-676.